Supporting Information

Ferreon et al. 10.1073/pnas.0811023106

SI Text

Purification of HDM2 (6–125). Cells were sonicated in 25 mM Tris·HCl, pH 8.0, 5 mM DTT, 1 mM PMSF. Soluble protein was purified by ion-exchange chromatography on HiTrap SP (GE Healthcare) in 20 mM Tris·HCl, pH 7.0, 2 mM DTT using a linear gradient of NaCl from 0 to 600 mM, followed by gel-filtration on Superdex 75 (GE Healthcare) in 20 mM Tris·HCl, pH 6.8, 150 mM NaCl, 1 mM DTT.

Preparation and Purification of Labeled p53 TAD Constructs. Constructs for p53 (13–37), p53 (38–61), and p53 (13–61) were generated by PCR-based mutagenesis of the full-length human p53 TAD. All p53 TAD constructs were expressed as N-terminal fusions with His_6-GB1 (residues 1–56 of the B1 domain of protein G) in *E. coli* BL21(DE3)[DNAY]. A glycine was inserted at the N terminus of p53 (13–61) and p53 (38–61) to facilitate thrombin cleavage. Additional residues (GSHMG) were introduced at the N terminus of p53 (13–37) during cloning to facilitate cleavage of the fusion protein. Pellets containing unlabeled, ^{15}N-labeled and (^{15}N,^{13}C) double-labeled p53 TAD peptides were suspended in 40 mL of 6 M urea, 25 mM Tris·HCl, pH 8.0, 150 mM NaCl, per liter of culture. The soluble fraction was isolated by centrifugation at 20,000 $\times$ *g* for 30 min. The supernatant was purified by chromatography on Ni-NTA resin and the His_6-GB1 tag was removed by thrombin digestion in the column. The cleaved p53 constructs were further purified by reversed phase HPLC.

Isothermal Titration Calorimetry. Isothermal titration calorimetry was performed using a MicroCal Omega VP-ITC instrument. Proteins were dialyzed against 20 mM Tris, 50 mM NaCl, 1 mM DTT, pH 8.0, except for KIX, which was dialyzed against 50 mM Tris, 50 mM NaCl, pH 7.0 to prevent aggregation. Experiments were performed at 35 °C. The typical concentration of p53 constructs (syringe) ranged from 300 to 800 μM and for the CBP domains and HDM2 (cell) 30–70 μM. Peptide concentrations were determined by absorbance at 280 nm. A typical ITC experiment consisted of 1 injection of 5 μL, followed by 29 injections of 10 μL up to a 2.5-fold molar excess of titrant. The heat of dilution is usually small and was subtracted from the calorimetric data, which were analyzed using a single-site binding model in MicroCal™ Origin. The stoichiometry ranged from 0.8 to 1.2, with most close to 1.0. Errors in K_d were estimated from duplicate or triplicate measurements.

NMR Spectroscopy. NMR spectra were recorded using Bruker 500, 600, 750, 800, and 900 MHz spectrometers and analyzed using NMRPipe (1) and NMRView (2). Backbone resonances of the free p53 TAD were assigned using standard 3D NMR experiments (3). Published backbone assignments for free CBP KIX (4), TAZ2 (5), TAZ1 (6) and NCBD (7) domains were used. The backbone resonances of p53 complexed to HDM2 and the CBP domains, and of the CBP domains in complex with p53 TAD, were assigned either by following fast exchange cross peaks in HSQC titrations and/or from triple resonance experiments. For the p53 TAD:HDM2 complex, assignments were obtained from 3D HNCA (8) and ^{15}N NOESY-HSQC spectra (9) and, for the ternary complexes, from chemical shift changes from the binary p53 TAD:HDM2 complexes.

NMR HSQC Titration Conditions. ^{1}H-^{15}N HSQC titrations were used to characterize binding of CBP domains to the p53 TAD constructs. The following protein titrations, mole ratio titration points, protein concentrations, buffer conditions and NMR field strength were used.

TAZ2-p53. 20 mM Mes, 75 mM NaCl, 1 mM DTT, pH 6.8, 35 °C, 800 MHz.

^{15}N p53 (13–61), ^{15}N p53 (13–37), ^{15}N p53 (38–61) were titrated with unlabeled TAZ2 - 1:0 (200:0 μM), 1:0.06 (196:11 μM), 1:0.1 (191:22 μM), 1:0.2 (183:42 μM), 1:0.5 (166:85 μM),1:1.1 (140:150 μM).

^{15}N TAZ2 was titrated with unlabeled p53 (13–37)–1:0 (150:0 μM), 1:0.65 (139:91 μM), 1:1.3 (129:170 μM), 1:5.2 (91:482 μM).

^{15}N TAZ2 was titrated with unlabeled p53 (38–61)–1:0 (150:0 μM), 1:0.65 (129:85 μM), 1:1.3 (114:149 μM), 1:2.6 (92:240 μM), 1:8 (50:400 μM).

^{15}N TAZ2 was titrated with unlabeled p53 (13–61)–1:0 (150:0 μM), 1:0.08 (147:11 μM), 1:0.23 (140:32 μM), 1:1 (115:115 μM).

NCBD-p53. 10 mM Sodium phosphate, 50 mM NaCl, pH 6.5, 25 °C, 600 MHz.

^{15}N p53 (13–61):NCBD–1:0 (100:0 μM), 1:0.5 (100:50 μM),1:1 (100:100 μM), 1:2 (100:200 μM).

^{15}N NCBD titrated with unlabeled p53 (14–28), p53 (38–61), p53 (13–61) - 1:0 (100:0 μM), 1:0.1 (100:10 μM),1:0.5 (100:50 μM),1:1 (100:100 μM), 1:2 (100:200 μM).

KIX-p53. 20 mM Tris, 50 mM NaCl, pH 6.5, 27 °C, 500 MHz.

^{15}N p53 (13–61):KIX - 1:0 (200:0 μM), 1:0.25 (194:48 μM),1:0.5 (188:94 μM),1:0.75 (182:137 μM), 1:1 (172:215 μM), 1:1.25 (172:215 μM), 1:1.5 (168:251 μM).

^{15}N KIX titrated with unlabeled p53 (14–28), p53 (38–61), p53 (13–61) - 1:0 (200:0 μM), 1:0.25 (184:92 μM),1:0.75 (177:133 μM), 1:1 (170:170 μM), 1:1.25 (164:205 μM), 1:1.5 (158:238 μM),1:2 (148:296 μM).

The NMR K_d determinations for TAZ1 and TAZ2 were conducted in 20 mM Tris, 50 mM NaCl, 1 mM DTT, pH 6.8 at 35 °C, and titrations were performed at 500 MHz.

^{15}N TAZ2:p53 (13–37) 1:0, 1:0.1, 1:0.2, 1:0.4, 1:0.6, 1:0.8, 1:1, 1:1.25, 1:1.5, 1:1.75, 1:2, 1:2.5, 1:3, 1:4, 1:4.5, 1:5. The concentration of ^{15}N TAZ2 was 200 μM for all titration points.

^{15}N TAZ2:p53 (38–61). 1:0 (200:0 μM), 1:0.1 (194:19 μM), 1:0.2 (189:38 μM), 1:0.4 (179:72 μM), 1:0.6 (171:102 μM), 1:0.8 (163:130 μM), 1:1 (156:156 μM), 1:1.25 (147:184 μM), 1:1.5 (140:210 μM), 1:1.75 (133:233 μM), 1:2 (127:254 μM), 1:2.5 (117:292 μM), 1:3 (108:323 μM), 1:3.5 (100:350 μM), 1:4 (93:373 μM), 1:6 (74:442 μM).

^{15}N TAZ1:p53 (38–61). 1:0 (200:0 μM), 1:0.1 (194:19 μM), 1:0.2 (189:38 μM), 1:0.4 (179:72 μM), 1:0.6 (171:102 μM), 1:0.8 (163:130 μM), 1:1 (156:156 μM), 1:1.25 (147:184 μM), 1:1.5 (140:210 μM), 1:1.75 (133:233 μM), 1:2 (127:254 μM), 1:2.5 (117:292 μM), 1:3 (108:323 μM), 1:3.5 (100:350 μM), 1:4 (93:373 μM), 1:6 (74:442 μM).

^{15}N TAZ2:p53 (13–61). 1:0 (200:0 μM), 1:0.1 (194:19 μM), 1:0.2 (189:38 μM), 1:0.4 (179:72 μM), 1:0.6 (171:102 μM), 1:0.8 (163:130 μM), 1:1 (156:156 μM), 1:1.25 (147:184 μM), 1:1.5 (140:210 μM), 1:1.75 (133:233 μM), 1:2 (127:254 μM), 1:2.5 (117:292 μM), 1:3 (108:323 μM), 1:3.5 (100:350 μM), 1:4 (93:373 μM)

^{15}N TAZ2:p53 (13–57)pT18. 1:0 (200:0 μM), 1:0.1 (194:19 μM), 1:0.2 (189:38 μM), 1:0.4 (179:72 μM), 1:0.6 (171:102 μM), 1:0.8 (163:130 μM), 1:1 (156:156 μM), 1:1.25 (147:184 μM), 1:1.5 (140:210 μM), 1:1.75 (133:233 μM), 1:2 (127:254 μM), 1:2.5 (117:292 μM), 1:3 (108:323 μM), 1:3.5 (100:350 μM), 1:4 (93:373 μM)

^{15}N TAZ1:p53 (13–61). 1:0 (200:0 μM), 1:0.1 (194:19 μM), 1:0.2 (189:38 μM), 1:0.4 (179:72 μM), 1:0.6 (171:102 μM), 1:0.8 (163:130 μM), 1:1 (156:156 μM), 1:1.25 (147:184 μM), 1:1.5 (140:210 μM), 1:1.75 (133:233 μM), 1:2 (127:254 μM), 1:2.5 (117:292 μM), 1:3 (108:323 μM), 1:3.5 (100:350 μM), 1:4 (93:373 μM)

^{15}N TAZ1:p53 (13–57)pS15pT18pS20. 1:0 (200:0 μM), 1:0.1 (194:19 μM), 1:0.2 (189:38 μM), 1:0.4 (179:72 μM), 1:0.6 (171:102 μM), 1:0.8 (163:130 μM), 1:1 (156:156 μM), 1:1.25 (147:184 μM), 1:1.5 (140:210 μM), 1:1.75 (133:233 μM), 1:2 (127:254 μM), 1:2.5 (117:292 μM), 1:3 (108:323 μM), 1:3.5 (100:350 μM), 1:4 (93:373 μM)

^{15}N TAZ1:p53 (13–37). 1:0 (200:0 μM), 1:0.1 (197:20 μM), 1:0.2 (195:39 μM), 1:0.4 (190:76 μM), 1:0.6 (185:111 μM), 1:0.8 (181:145 μM), 1:1 (176:176 μM), 1:1.25 (171:214 μM), 1:1.5 (167:250 μM), 1:1.75 (162:284 μM), 1:2 (158:316 μM), 1:2.5 (150:375 μM), 1:3 (143:429 μM), 1:4 (130:522 μM), 1:6 (111:667 μM), 1:8 (97:774 μM).

For the ternary complexes, separate NMR samples (p53 (13–61) alone, binary complex p53:HDM2, ternary complex HDM2:p53:CBP) were prepared with same buffer conditions as the CBP:p53 titrations, 25 °C, 800 MHz: The protein concentrations are as follows:

NCBD:p53:HDM2 complex, 300 μM each; KIX:p53:HDM2, 150 μM each; TAZ2:p53:HDM2 and TAZ1:p53:HDM2, 200 μM.

For K_d determination (Fig. S9*B*) of the ^{15}N p53 (38–61) titrated with TAZ2, 1:0 (100:0 μM), 1:0.1 (98:10 μM), 1:0.25 (95:24 μM), 1:0.4 (91:37 μM), 1:0.55 (89:49 μM), 1:0.7 (87:61 μM), 1:0.85 (84:71 μM), 1:1 (82:82 μM).

For AD2 titration with TAZ2 in the binary complex p53 (13–61):HDM2, ^{15}Np53 (13–61):HDM2 binary complex at 100 μM each, were titrated with unlabeled TAZ2- 1:1:0 (100:100:0 μM), 1:1:0.1 (98:98:10 μM), 1:1:0.25 (95:95:24 μM), 1:1:0.4 (91:91:37 μM), 1:1:0.55 (89:89:49 μM), 1:1:0.7 (87:87:61 μM), 1:1:0.85 (84:84:71 μM), 1:1:1 (82:82:82 μM).

Pulldown Experiments. For pulldown experiments, the p53-binding domain of HDM2 (residues 17–125) was expressed with N-terminal His_6 and GB1 fusion tags. Expression of His_6GB1-HDM2 in BL21 DE3 [DNAY] was induced at 15 °C for 16 h and soluble protein was isolated by metal affinity chromatography on Ni-NTA resin (Qiagen). His_6GB1-HDM2 was further purified by ion exchange chromatography on HiTrap SP (GE Healthcare) in 20 mM Tris pH 7.2, 1 mM DTT using a gradient to 600 mM NaCl. p53 (1–94) was expressed and purified in similar fashion to that described for p53 (13–61). All proteins for pulldown experiments were exchanged into 20 mM Tris, 50 mM NaCl, 1 mM DTT (pH 7.5 for p53 and TAZ1, pH 7 for HDM2). His_6GB1 produced by thrombin cleavage of His_6GB1-p53 was used as a control for nonspecific binding.

For each pulldown assay, 30 μL of IgG Sepharose 6 Fast Flow (GE Healthcare) was equilibrated in assay buffer (20 mM Tris pH 7, 50 mM NaCl, 0.1% IGEPAL CA-630) and loaded with 6 nmol of His_6GB1-HDM2. Resin-bound His_6GB1-HDM2 was incubated with 6 nmol of p53 (1–94) and/or CBP TAZ1 for 20 min at room temperature. Unbound proteins were removed by washing with assay buffer. Bound proteins were eluted from the resin by addition of 0.1% trifluoroacetic acid and monitored by reversed phase HPLC chromatography on a Jupiter 5 μm C4 analytical column (Phenomenex). A second set of control experiments was performed with His_6GB1 in place of His_6GB1-HDM2.

NMR Titration Experiments Can Accurately Estimate Small K_{d1} Value for Two-Site Binding. To accurately estimate the dissociation constant K_d from NMR titration experiments, the protein concentration should be close to the K_d of the protein-ligand interaction. Fig. S1*A* shows the simulation of titration curves for 1-site binding with a protein concentration of 200 μM, which is typical for NMR measurements, assuming a K_d of 1 nM (red), 10 nM (orange), 100 nM (green), 1 μM (blue), and 5 μM (black). The fraction of the bound form, f_B, was calculated using the following equation:

$$f_B = \frac{1}{2}\{([P]_0 + [L]_0 + K_d) - \sqrt{([P]_0 + [L]_0 + K_d)^2 - 4[P]_0[L]_0}\}$$

where $[P]_0$ and $[L]_0$ are the total concentrations of protein and ligand, respectively (3, 10). The titration curves with a K_d of <100 nM are indistinguishable, showing that it is not possible to determine such a small K_d value by NMR titration experiments, if there is only a single binding site.

In contrast, there is a dramatic change in the titration curves in the case of 2-site binding. Fig. S1*B* shows the simulation of titration curves for 2-site binding with a protein concentration of 200 μM and with a K_{d2} of 10 μM, which was observed for the TAZ2-AD2 interactions (see Table 1). The color codes are the same as those for Fig. S1*A*. The occupancies of the primary and secondary binding sites, f_1 and f_2, are shown by thick continuous lines and by thin continuous lines with circles, respectively. f_1 and f_2 were calculated using the following equations:

$$f_1 = \frac{[L]}{K_{d1} + [L]}$$

$$f_2 = \frac{[L]}{K_{d2} + [L]}$$

where $[L]$ is a free ligand concentration, which is a solution of the following cubic equation and contains K_{d1}, K_{d2}, $[P]_0$, and $[L]_0$ in its closed form (11):

$$[L]^3 + (2[P]_0 - [L]_0 + K_{d1} + K_{d2})[L]^2 + \{([P]_0 - [L]_0)(K_{d1} + K_{d2}) + K_{d1}K_{d2}\}[L] - K_{d1}K_{d2}[L]_0 = 0$$

Fig. S1*B* clearly shows that the curves for f_1, which is comparable with f_B for 1-site binding, are much more sensitive to the changes in K_{d1} even at a K_{d1} of <100 nM. This situation is different from 1-site binding. The rationale for this difference is as follows. In 2-site binding, secondary binding can start before primary binding is saturated if secondary binding is relatively tight (see the curves for f_2 in Fig. S1*B*). Then, the primary site is not fully occupied at ≈1:1 protein:ligand ratio, resulting in smaller f_1 (for 2-site binding) than f_B (for 1-site binding). Thus, the presence of secondary binding enhances the difference in the occupancy of the primary site. As a consequence, we can reliably estimate a K_{d1} that is <100 nM by NMR titration experiments.

However, if the secondary binding is very weak, it is not possible to accurately determine K_{d1}, because the binding events approach 1-site binding. To estimate the ranges of K_{d1} and K_{d2} that allow accurate K_d determination, we simulated titration curves with various K_{d1} and K_{d2} values and investigated which sets of K_{d1} and K_{d2} can be reproduced by global fitting. The details of the simulation will be described elsewhere. In brief, the titration curves were generated using the Δδ histogram of ^{15}N-labeled TAZ2 titration with AD1 (73 peaks, 146 curves) and assuming that the K_{d1} and K_{d2} values are powers of 10 between 10^{-10} and 10^{-1} M (see the grid points in Fig. S1*C*; $K_{d1} \leq K_{d2}$). A small amount of noise was added to each data point to simulate actual NMR data. Then, a global fit was performed for each K_d set as described in Materials and Methods and the fitted K_d values were compared with those used to generate the titration

curves. In Fig. S1*C*, the red, orange, and green squares and the cross symbols show that both fitted K_d values and fitting errors are <5%, 5–10%, 10–20%, or >20%, respectively, from the input K_d values used for generating the curves. The gray circles and diamonds show parameter sets for which only K_{d1} or K_{d2} could be accurately obtained by global fitting because the binding events approach 1-site binding at higher K_{d2} or at lower K_{d1}, respectively. The simulation results show clearly that K_{d1} values in the range of 10 nM to 1 μM can be reliably obtained by global fitting if K_{d2} is between 10 and 1,000-fold larger than K_{d1} (red and orange regions in Fig. S1*C*). All sets of K_{d1} and K_{d2} in Table 1 lie within the red regions of Fig. S1*C*, showing that the K_d values obtained from NMR titrations in this work are reliable and accurate.

1. Delaglio F, et al. (1995) NMRPipe: A multidimensional spectral processing system based on UNIX pipes. *J Biomol NMR* 6:277–293.
2. Johnson BA, Blevins RA (1994) NMRView: A computer program for the visualization and analysis of NMR data. *J Biomol NMR* 4:604–613.
3. Cavanagh J, Fairbrother WJ, Palmer AG, III, Rance M, Skelton NJ (2007) *Protein NMR Spectroscopy: Principles and Practice* (Elsevier Academic, Burlington MA).
4. Radhakrishnan I, et al. (1999) Structural analyses of CREB-CBP transcriptional activator-coactivator complexes by NMR spectroscopy: Implications for mapping the boundaries of structural domains. *J Mol Biol* 287:859–865.
5. De Guzman RN, Liu HY, Martinez-Yamout M, Dyson HJ, Wright PE (2000) Solution structure of the TAZ2 (CH3) domain of the transcriptional adaptor protein CBP. *J Mol Biol* 303:243–253.
6. De Guzman RN, Wojciak JM, Martinez-Yamout MA, Dyson HJ, Wright PE (2005) CBP/p300 TAZ1 domain forms a structured scaffold for ligand binding. *Biochemistry* 44:490–497.
7. Ebert MO, Bae SH, Dyson HJ, Wright PE (2008) NMR Relaxation study of the complex formed between CBP and the activation domain of the nuclear hormone receptor coactivator ACTR. *Biochemistry* 47:1299–1308.
8. Grzesiek S, Bax A (1992) Improved 3D triple-resonance NMR techniques applied to a 31 kDa protein. *J Magn Reson* 96:432–440.
9. Zuiderweg ERP, Fesik SW (1989) Heteronuclear three-dimensional NMR spectroscopy of the inflammatory protein C5a. *Biochemistry* 28:2387–2391.
10. Fielding L (2007) NMR methods for the determination of protein-ligand dissociation constants. *Prog NMR Spectros* 51:219–242.
11. Wang ZX, Jiang RF (1996) A novel two-site binding equation presented in terms of the total ligand concentration. *FEBS Lett* 392:245–249.

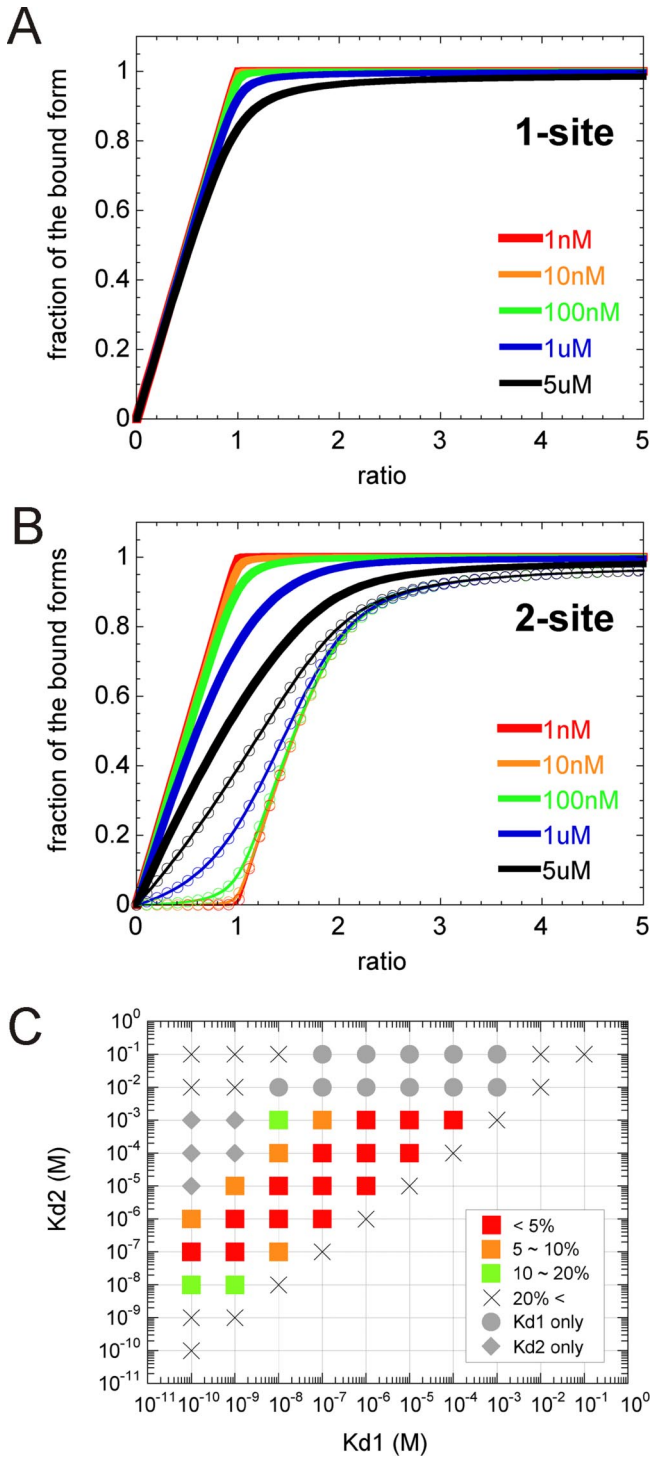

Fig. S1. (*A*) Simulation of titration curves for 1-site binding with a protein concentration of 200 μM, which is typical for NMR measurement, assuming a K_d of 1 nM (red), 10 nM (orange), 100 nM (green), 1 μM (blue), and 5 μM (black). (*B*) Simulation of titration curves for 2-site binding with a protein concentration of 200 μM and with a K_{d2} of 10 μM (as observed for the TAZ2-AD2 interactions; Table 1). The color codes are the same as those for part A. The occupancies of the primary and secondary binding sites, f_1 and f_2, are shown by thick continuous lines and by thin continuous lines with circles, respectively. (*C*) Grid showing a comparison of titration curves generated using the $\Delta\delta$ histogram of ^{15}N-labeled TAZ2 titration with AD1 (73 peaks, 146 curves) and assuming that the K_{d1} and K_{d2} values are power of 10 between 10^{-10} and 10^{-1} M. A small noise factor was added to each data point to simulate actual data. A global fit was performed for each K_d set as described in Methods, and the fitted K_d values were compared with those used in generating the titration curves. The red, orange, and green squares and cross symbols show that both fitted K_d values and fitting errors are $<$5%, 5–10%, 10–20%, and $>$20%, respectively, of the K_d values used for generating the curves. Gray circles and diamonds show that only K_{d1} or K_{d2} were accurately obtained by the global fit, because the binding events approached 1-site binding at higher K_{d2} or at lower K_{d1}, respectively.

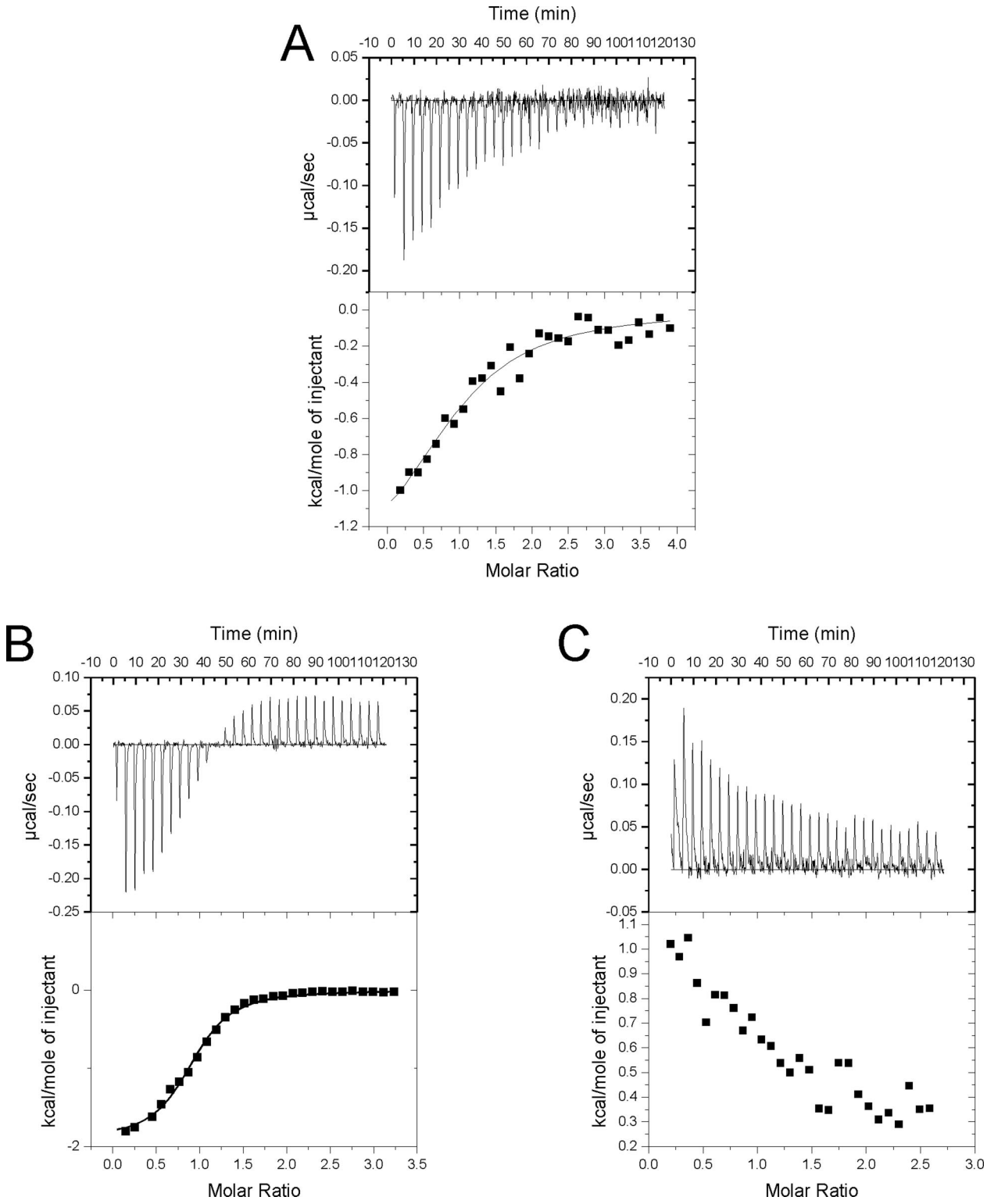

Fig. S2. Isothermal titration calorimetry (ITC) data for titration of KIX with p53. (*A*) *KIX* + *p53*(13–61) [$n = 1.0 \pm 0.1$; $K = 6.0 \pm 1.8 \times 10^4$; $\Delta H = -1{,}606 \pm 294$ kcal·mol^{-1}; $\Delta S = 16.7$ cal·mol^{-1}·K^{-1}]. (*B*) KIX + p53 (13–57), phosphorylated at S15, T18 and S20 [$n = 0.92 \pm 0.13$; $K = 4.0 \pm 0.4 \times 10^5$; $\Delta H = -1{,}908 \pm 37$ kcal·mol^{-1}; $\Delta S = 19.5$ cal·mol^{-1}·K^{-1}]. (*C*) Control (dilution only) p53 (13–57), phosphorylated at S15, T18 and S20.

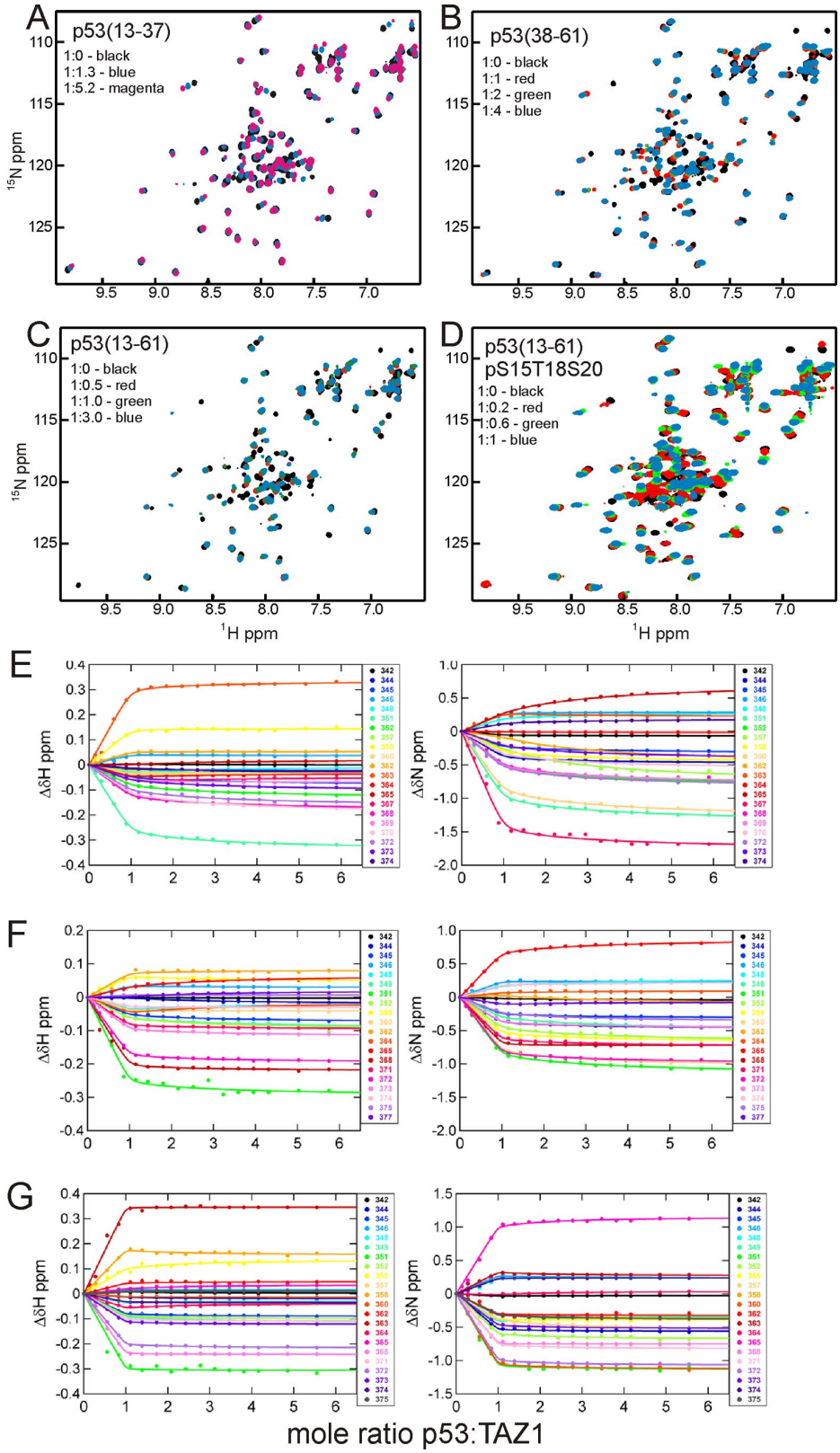

Fig. S3. (*A–D*) Titration of ^{15}N TAZ1 with unlabeled p53. (*A*) p53 (13–37). (*B*) p53 (38–61). (*C*) p53 (13–61). (*D*) p53 (13–57) phosphorylated at S15, T18, S20. (*E–G*) Selection of data from global fits of ^{1}H (*Left*) and ^{15}N (*Right*) chemical shift changes of HSQC cross peaks of ^{15}N TAZ1 as a function of the ratio of p53:TAZ1. Only the peaks showing clear fast-exchange shifts were used for fitting. (*E*) p53 (13–61). (*F*) p53 (13–57)pT18. (*G*) p53 (13–57)pS15pT18pS20.

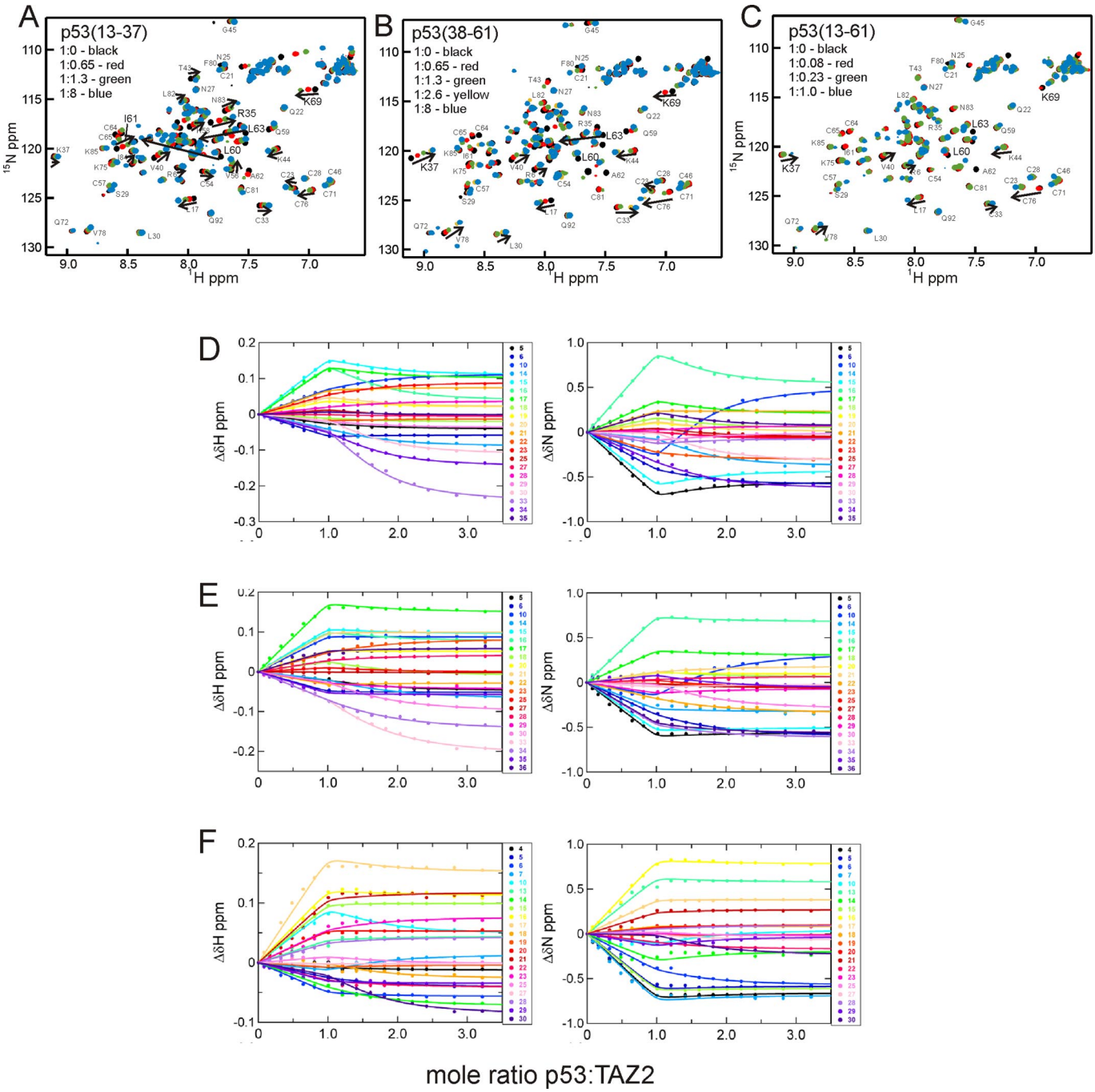

Fig. S4. (*A*–*C*) Titration of ^{15}N TAZ2 with unlabeled p53. (*A*) p53 (13–37). (*B*) p53 (38–61). (*C*) p53 (13–61). (*D*–*F*) Global fitting of ^{1}H (*Left*) and ^{15}N (*Right*) chemical shift changes as a function of the ratio of p53:TAZ2. Only the peaks showing clear fast-exchange shifts were used for fitting. (*D*) p53 (13–61). (*E*) p53 (13–57)pT18. (*F*) p53 (13–57)pS15pT18pS20.

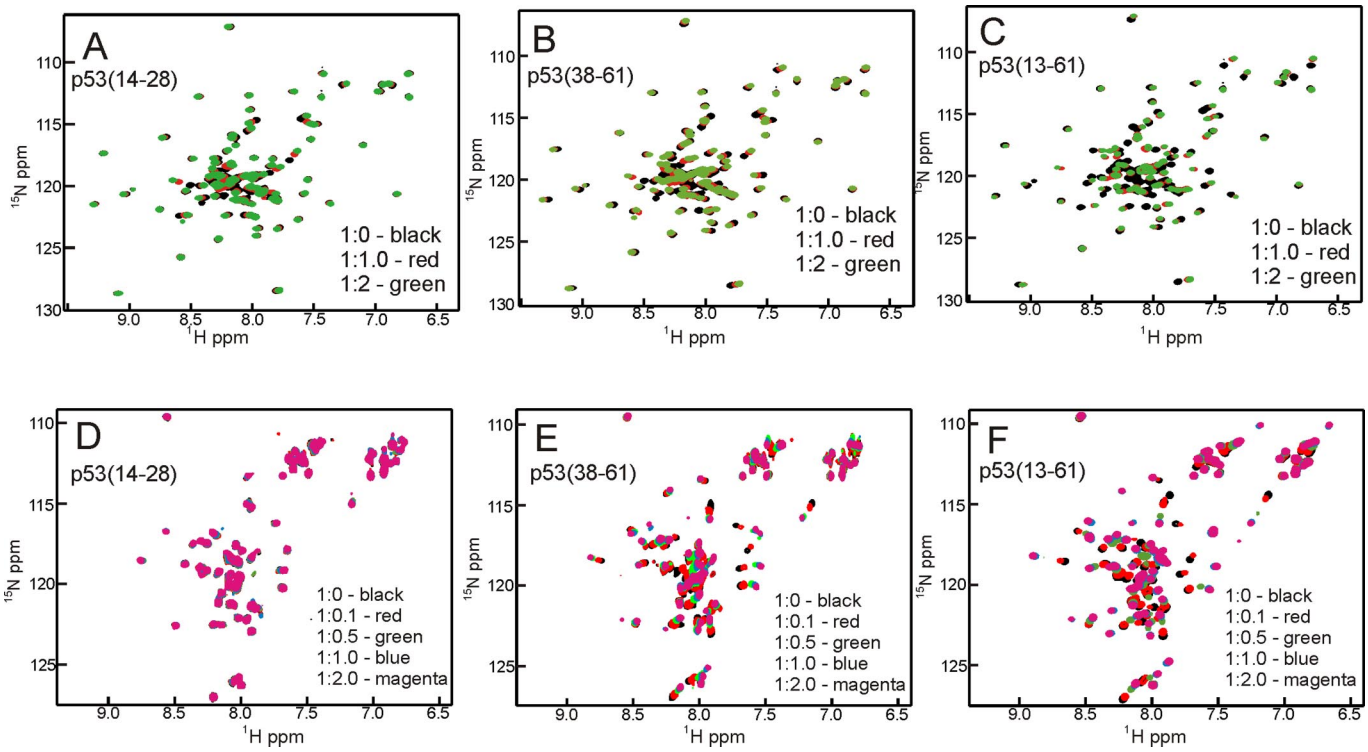

Fig. S5. (*A–C*) Titration of ^{15}N KIX with unlabeled p53. (*A*) p53 (14–28). (*B*) p53 (38–61). (*C*) p53 (13–61). (*D–F*) Titration of ^{15}N NCBD with unlabeled p53. (*D*) p53 (14–28). (*E*) p53 (38–61). (*F*) p53 (13–61).

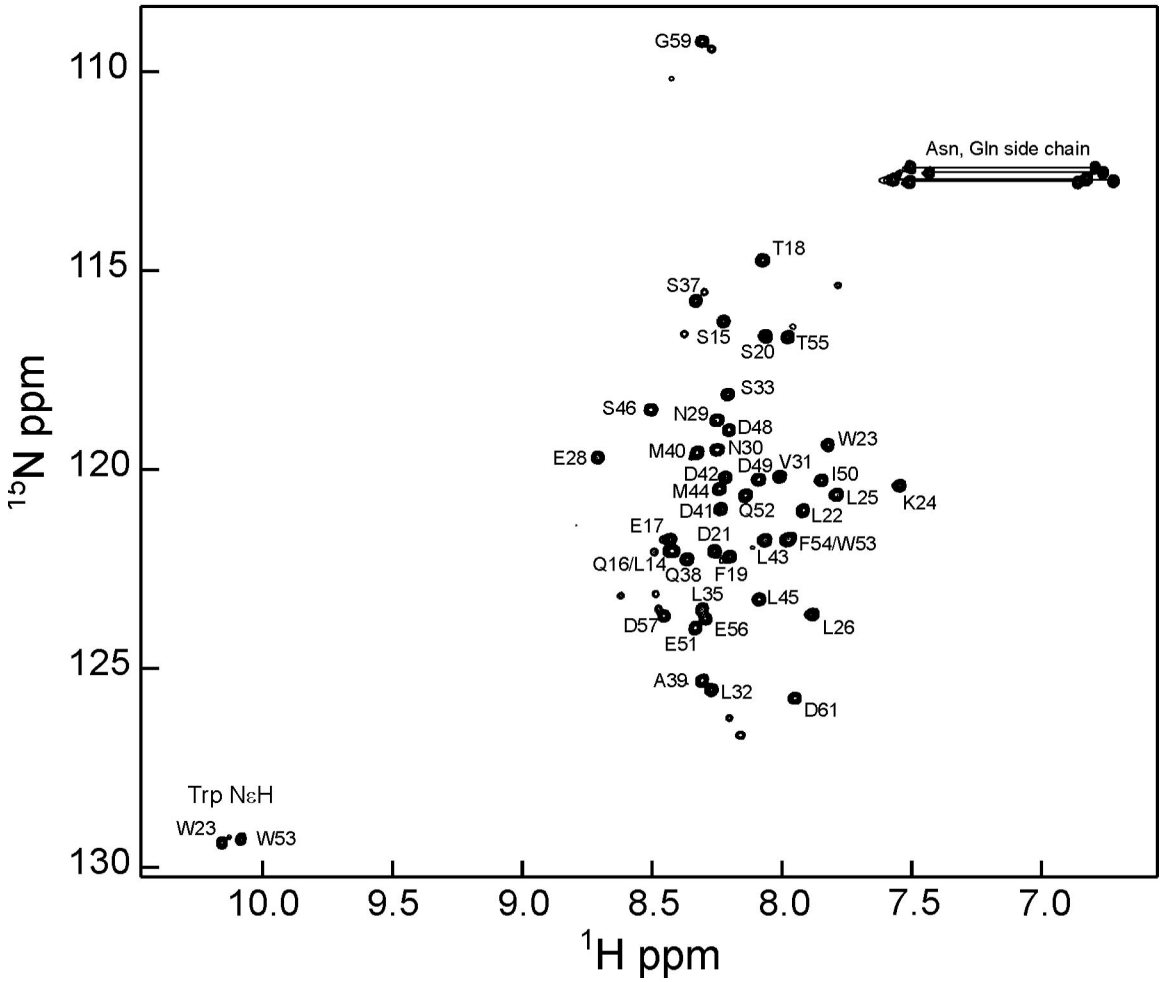

Fig. S6. ^{1}H-^{15}N HSQC spectrum of p53 (13–61) at 25 °C in 10 mM sodium phosphate, 50 mM NaCl at pH 6.5.

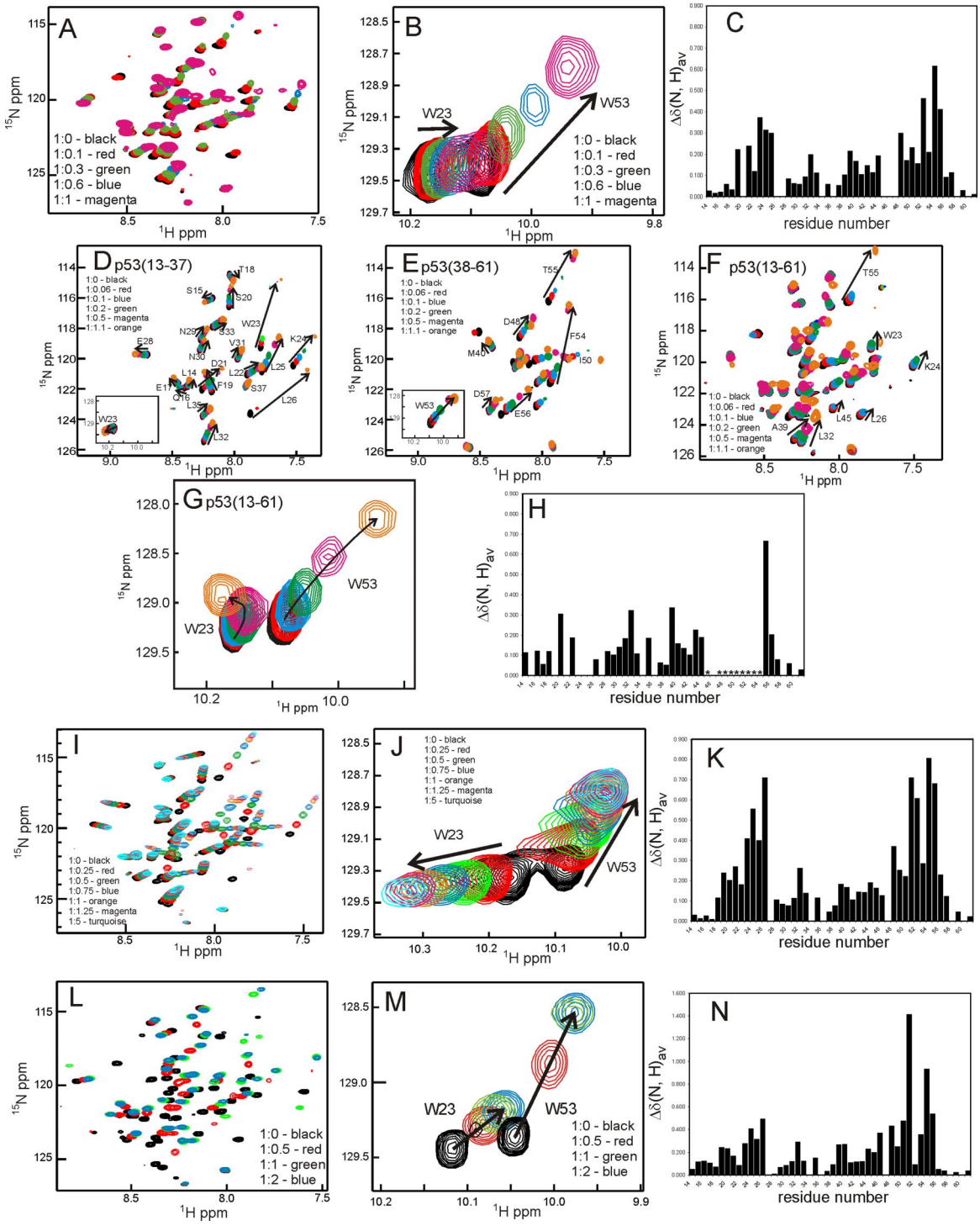

Fig. S7. ^{15}N p53 peptides titrated with unlabeled TAZ1 (*A–C*), TAZ2 (*D–H*), KIX (*I–K*) and NCBD (*L–N*). (*A*) ^{15}N p53 (13–61) with TAZ1, backbone NH region. (*B*) ^{15}N p53 (13–61) with TAZ1, Trp side chain region. (*C*) average chemical shift difference between p53 (13–61) amide resonances in the presence and absence of TAZ1. (*D*) ^{15}N p53 (13–37) with TAZ2, backbone region with inset Trp side chain region. (*E*) ^{15}N p53 (38–61) with TAZ2, backbone region with inset Trp side chain region. (*F*) ^{15}N p53 (13–61) with TAZ2, backbone region. (*G*) ^{15}N p53 (13–61) with TAZ2, Trp side chain region. (*H*) Average chemical shift difference between p53 (13–61) amide resonances in the presence and absence of TAZ2. (*I*) ^{15}N p53 (13–61) titrated with unlabeled KIX, backbone NH region. (*J*) ^{15}N p53 (13–61) titrated with unlabeled KIX, Trp side chain region. (*K*) Average chemical shift difference between p53 (13–61) amide resonances in the presence and absence of KIX. (*L*) ^{15}N p53 (13–61) titrated with unlabeled NCBD, backbone NH region. (*M*) ^{15}N p53 (13–61) titrated with unlabeled NCBD, Trp side chain region (same as Fig. 3*A*). (*C*) average chemical shift difference between p53 (13–61) amide resonances in the presence and absence of NCBD. In *C*, *H*, *K*, and *N*, $\Delta\delta(N,H)_{av} = \{\Delta\delta(H)^2 + [\Delta\delta(N)/5]^2\}^{½}$.

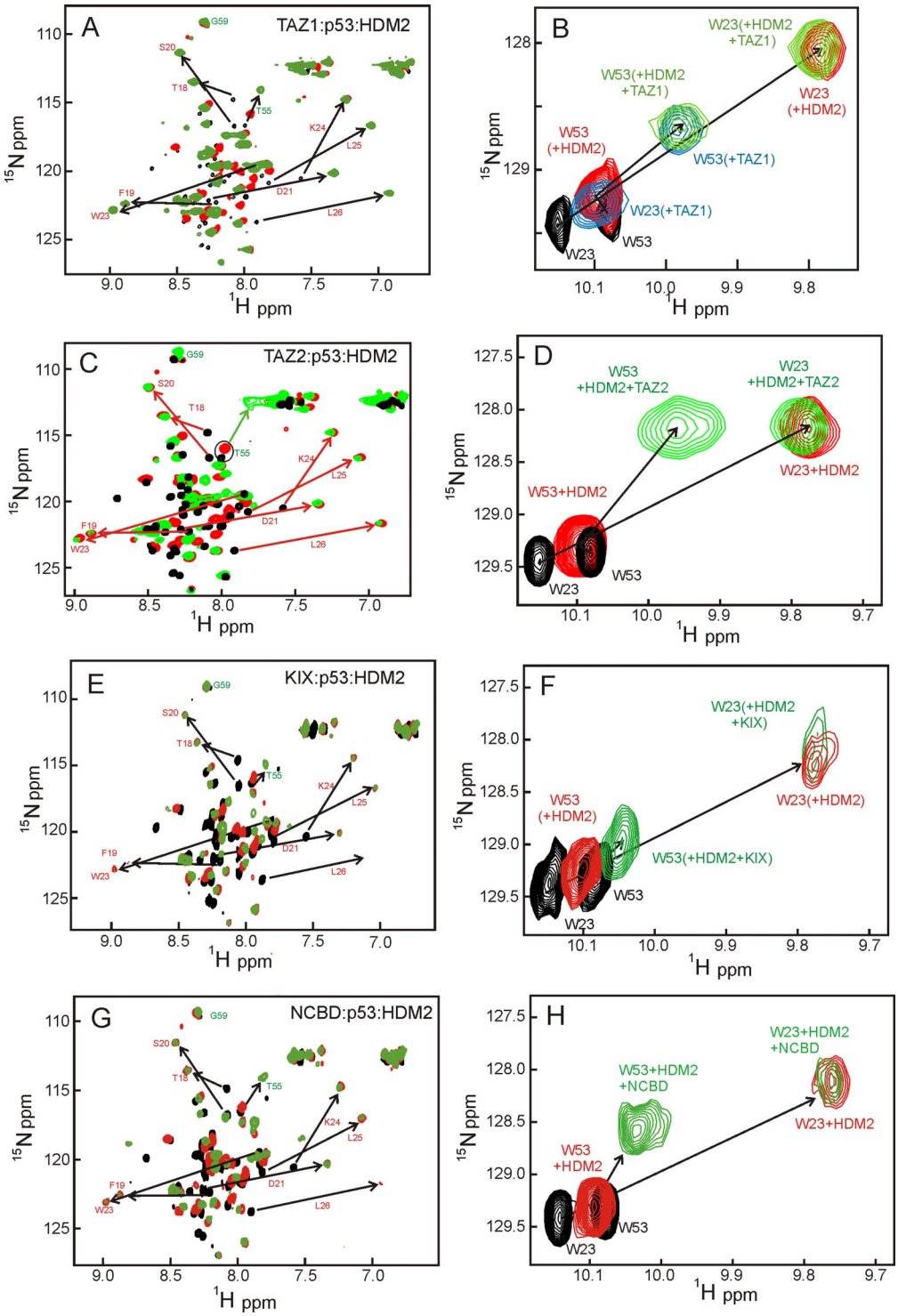

Fig. S8. ^{15}N p53 (13–61) (black) + 1:1 HDM2 (6–125) (red) and with further addition of an equimolar amount of CBP domains (green). (*A*) ^{15}N p53 (13–61) backbone amides with HDM2 and TAZ1. (*B*) ^{15}N p53 (13–61) Trp side chain amides with HDM2 and TAZ1. Blue: Trp side chain signals observed for a 1:1 complex of ^{15}N p53 (13–61) with unlabeled TAZ1. (Same as Fig. 4*B*). (*C*) ^{15}N p53 (13–61) backbone amides with HDM2 and TAZ2 (Same as Fig. 4*A*). (*D*) ^{15}N p53 (13–61) Trp side chain amides with HDM2 and TAZ2. (*E*) ^{15}N p53 (13–61) backbone amides with HDM2 and KIX. (*F*) ^{15}N p53 (13–61) Trp side chain amides with HDM2 and KIX. (*G*) ^{15}N p53 (13–61) backbone amides with HDM2 and NCBD. (*H*) ^{15}N p53 (13–61) Trp side chain amides with HDM2 and NCBD.

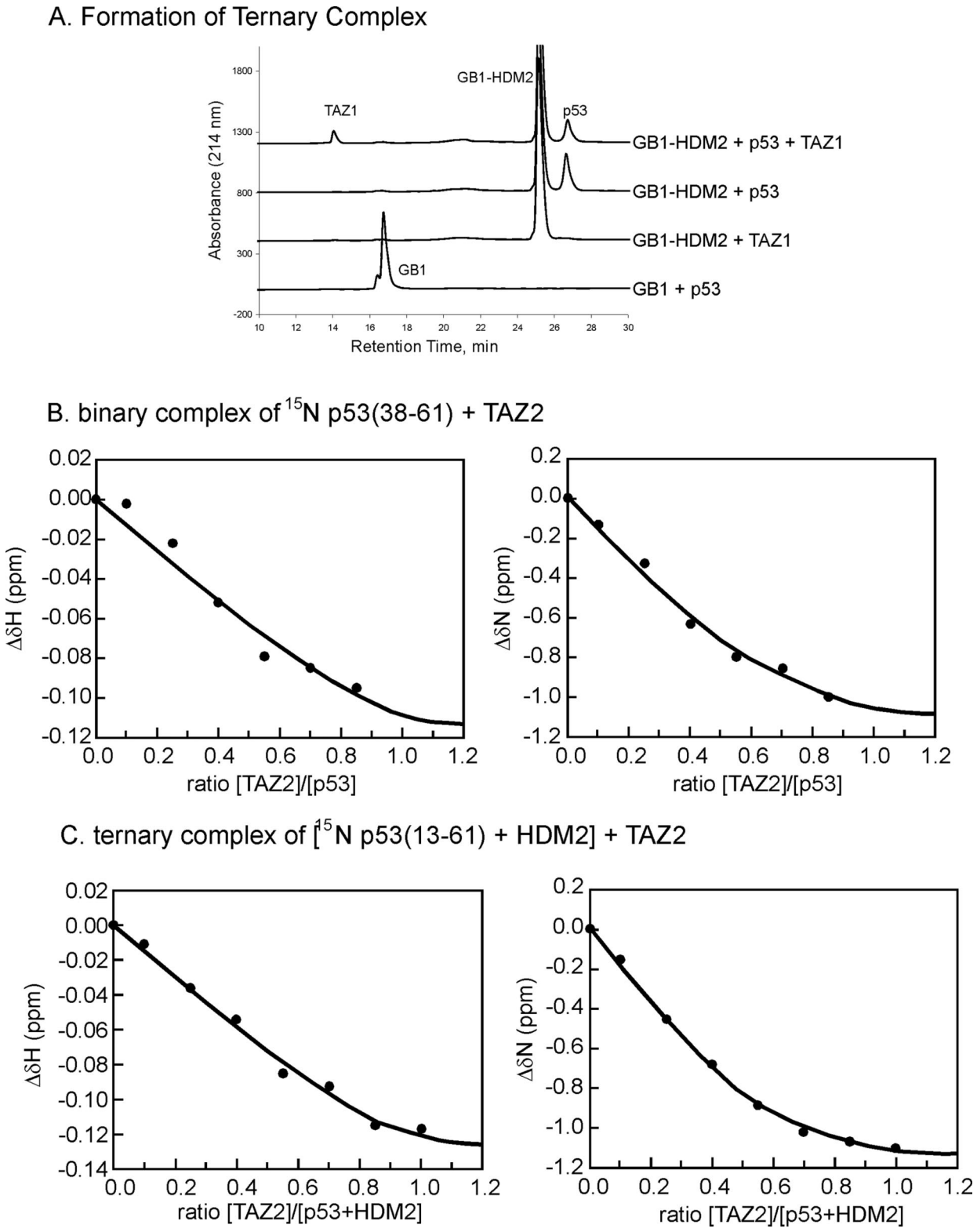

Fig. S9. (*A*) Demonstration of ternary HDM2:p53:TAZ1 complex formation by pulldown assay monitored by reversed phase HPLC. HDM2 bound to IgG Sepharose via an N-terminal GB1 (protein G, B1 domain) fusion tag pulls down a p53:TAZ1 complex (upper trace). Control experiments show that HDM2 does not directly interact with TAZ1 and that p53 specifically bridges the ternary HDM2:p53:TAZ1 complex, because it does not bind to IgG resin-bound GB1 fusion tag without HDM2 (lower 2 traces). (*B* and *C*), C. NMR titration showing changes in the chemical shift of the W53 side chain amide cross peak of ^{15}N p53 as TAZ2 is added in the mole ratios shown, to AD2 (residues 38–61) of p53. (*B*) and residues 13–61 of p53 in complex with HDM2 in a 1:1 ratio (*C*). All data were fitted to $K_{d1} = 55$ nM and $K_{d2} = 10.1$ μM from Table 1.